Synthesis and Structure of Cp^*_2TiH, $Cp^*_2TiH_2Li(tmed)$, and $[Cp^*_2TiOLi(THF)]_2$

Wayne W. Lukens, Jr., Phillip T. Matsunaga, and Richard A. Andersen*

Chemistry Department and Chemical Sciences Division of E. O. Lawrence Berkeley National Laboratory, University of California, Berkeley, California 94720

Received July 14, 1998

The solid-state crystal structure of the d^1 hydride Cp^*_2TiH shows that it has a bent sandwich structure with an open Cp*(centroid)−Ti−Cp*(centroid) angle of 150°. The crystal structure contains two molecules in the asymmetric unit, and the hydridic hydrogen atom is located and refined with isotropic thermal parameters to a Ti−H distance of 1.69(5) and 1.84(4) Å in each independent molecule; the average Ti−H distance is 1.76 Å. In each molecule, the Ti−H vector lies on the idealized C_2 axis of the bent metallocene. The addition of *n*-BuLi and $Me_2NCH_2CH_2NMe_2$ (tmed) in hexane to Cp^*_2TiH or the addition of $[Li(tmed)]_2C_{10}H_8$ to Cp^*_2TiCl gives the anionic dihydride $Cp^*_2Ti(\mu\text{-}H)_2Li(tmed)$. The hydride atoms are not located in the X-ray diffraction experiment, but electron paramagnetic resonance spectra show coupling to two equivalent hydrogen nuclei, $A_H^{iso} = 9.6$ G. In addition, coupling to ^7Li, confirmed by the preparation of the ^6Li isotopomer, shows that the unpaired electron couples with each hydridic hydrogen and lithium nucleus. The proposed structure has two hydride ligands bridging the Cp^*_2Ti and Li(tmed) fragments. Water in tetrahydrofuran (THF) reacts with $Cp^*_2Ti(\mu\text{-}H)_2Li(tmed)$ to give the dimer, $[Cp^*_2TiOLi(THF)]_2$. Its X-ray structure shows that the two Cp^*_2TiO fragments are joined together by the Li(THF) fragments such that the Li_2O_2 unit is a square as found in dimeric lithium alkoxides; in this case, the alkoxide is the metallocene $Cp^*_2TiO^-$. Variable-temperature magnetic susceptibility shows that the unpaired electrons on each $Cp^*_2TiO^-$ fragment are not coupled down to 5 K.

Introduction

The ground-state structure of trivalent metallocene hydrides of titanium is surrounded by controversy. This subject is part of the larger question about the nature of titanocene, which has been reviewed.[1] The initial report showed that the electron paramagnetic resonance (EPR) spectra of species derived from the reaction of Cp_2TiCl with an excess of β-hydride-containing alkyllithium or Grignard reagents gave ether solutions of the Ti(III) dihydride anions, $[Cp_2TiH_2]^-$.[2] In solution at room temperature, the isotropic *g* value is 1.992, and hyperfine couplings to the Ti−*H* and Cp−*H* atoms were 7 and 0.4 G, respectively. Later, frozen solution EPR spectra showed axial symmetry, and in some cases, coupling to the alkali metal cation was observed. For example, $A_{^7Li}^{iso}$ in Cp_2TiH_2Li·tetrahydrofuran (THF) is 2.3 G.[3] The interpretation of these data suggested that the unpaired electron occupies an orbital of a symmetry.

The subject of the constitution of the neutral metallocene hydrides of titanium is more complex. The initial report showed that Cp_2TiH exists in two forms: one violet and the other gray-green.[4] The violet form was postulated to be a dimer with symmetrical $Ti_2(\mu\text{-}H)_2$ bridge bonds similar to the halide-bridged dimers.[5] The recently reported X-ray crystal structure of the *ansa*-indenyl derivative is probably a good structural model for the violet form.[6] The gray-green form is thought to be polymeric, and its structural details are unknown.

The use of Cp* (Me_5C_5) in place of Cp greatly simplified the problem. Cp^*_2TiH was first mentioned to result from the decomposition of $Cp^*_2TiMe_2$,[7] but a better synthesis is the reaction of Cp^*_2TiMe with hydrogen.[8] In solution at room temperature, Cp^*_2TiH is monomeric and paramagnetic but EPR silent, and the Cp* resonances in the ^1H NMR spectrum obey the Curie law.[7] The ground-state structure of this simple metallocene hydride is unknown; it has been suggested that the molecule is in equilibrium with a fulvene−dihydride or −dihydrogen complex (eq 1). In addition, calculations on Cp_2TiH suggest that the hydride lies on[9] or off[10] the C_2 axis of the molecule. Recently, the crystal structure of the phenyl-substituted permethylmetallocene (Me_4-

* Address correspondence to this author at Chemistry Department, University of California, Berkeley, CA 94720.

(1) *Comprehensive Organometallic Chemistry* 1st ed.; Wilkinson, G., Ed.; Pergamon Press: New York, 1982; Vol. 3, p 314.
(2) Brintzinger, H. H. *J. Am. Chem. Soc.* **1967**, *89*, 6871.
(3) Kenworthy, J. G.; Hyatt, J.; Symons, M. C. R. *J. Chem. Soc. A* **1971**, 1020.
(4) Bercaw, J. E.; Brintzinger, H. H. *J. Am. Chem. Soc.* **1969**, *91*, 7301.
(5) (a) Jungst, R.; Sekutowski, D.; Davis, J.; Luly, M.; Stucky, G. *Inorg. Chem.* **1977**, *16*, 1645. (b) Coutts, S. P.; Wailes, P. C.; Martin, R. L. *J. Organomet. Chem.* **1973**, *53*, 1891.
(6) Xin, S.; Harrod, J. F.; Samuel, E. *J. Am. Chem. Soc.* **1994**, *116*, 11562.
(7) Bercaw, J. E. *J. Am. Chem. Soc.* **1974**, *96*, 5087.
(8) Luinstra, G. A.; Teuben, J. H. *J. Am. Chem. Soc.* **1992**, *114*, 3361.
(9) Bierwagen, E. P.; Bercaw, J. E.; Goddard, W. A., III. *J. Am. Chem. Soc.* **1994**, *116*, 1481.
(10) Lauher, J. W.; Hoffmann, R. *J. Am. Chem. Soc.* **1976**, *98*, 1729.

10.1021/om980601n CCC: $15.00
Publication on Web 10/16/1998

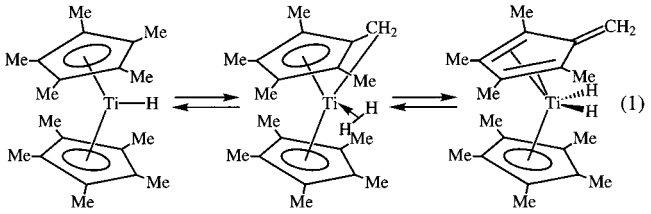

(1)

$PhC_5)_2TiH$ was published, and the hydride ligand was located on the C_2 axis of the molecule.[11]

In this manuscript, we describe the single-crystal structures of the parent metallocene, Cp*$_2$TiH, the dihydride anion, Cp*$_2$Ti(μ-H)$_2$Li·Me$_2$NCH$_2$CH$_2$NMe$_2$(tmed), and the product of its reaction with water, [Cp*$_2$TiOLi(THF)]$_2$.

Results and Discussion

Structure of Cp*$_2$TiH. The hydride was made, as previously reported, by stirring Cp*$_2$TiMe with dihydrogen (150 psi) in pentane.[7,8] Red plates were isolated by cooling a pentane solution to −40 °C. The ^{1}H NMR spectrum in toluene-d_8 at 30 °C shows a single resonance at δ = 22.6 ppm ($\nu_{1/2}$ = 128 Hz) due to the Cp* ligand in agreement with the earlier report.[7] The hydride behaves as a simple paramagnet in the solid state since a plot of $1/\chi_m$ as a function of temperature is linear from 5 to 100 K with $\mu_{eff} = 1.72\ \mu_B$. The hydride melts at 234−237 °C and gives a $[M - H]^+$ fragment in its mass spectrum.

In an attempt to prepare the deuteride, Cp*$_2$TiMe was exposed to dideuterium. All of the hydrogen atoms exchange with deuterium, giving $[(CD_3)_5C_5]_2TiD$.[7] This substitution allows the assignment of ν(Ti−D) at 1048 cm^{-1} and, therefore, the feature at 1490 cm^{-1} in Cp*$_2$TiH to ν(Ti−H). Similar values have been reported for $(Me_4PhC_5)_2TiH$: ν(Ti−D) = 1092 cm^{-1} and ν(Ti−H) = 1505 cm^{-1}.[11]

IR spectra of neutral metallocene hydride complexes of the 4d and 5d metals have been studied.[12] When this infrared spectroscopic study was published, Cp*$_2$VH[13b] was the only known 3d metallocene hydride, so periodic trends could not be extended to the first-row transition-metal hydrides. For the 4d and 5d metals, the stretching frequency increases down a column and across a row; this trend presumably mirrors the M−H bond strength. For the known 3d metallocene hydrides, a similar trend is followed: Cp*$_2$ScH(THF), ν(Sc−H) = 1390 cm^{-1};[13a] Cp*$_2$TiH, ν(Ti−H) = 1490 cm^{-1}; Cp*$_2$VH, ν(V−H) = 1625 cm^{-1}.[14b] These trends are perhaps best rationalized by noting that the size of the metal decreases and the ionization energy increases across the first row. This progression results in better overlap between the Cp*$_2$M and H fragment orbitals, and the orbital energies become closer together, yielding a stronger bond from left to right across the first row.

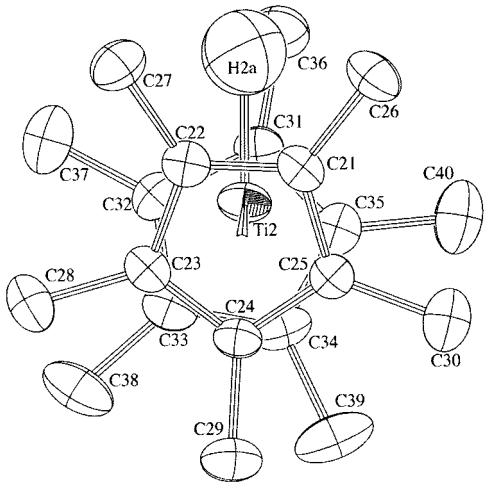

Figure 1. ORTEP diagram of Cp*$_2$TiH, 50% thermal ellipsoids, all atoms anisotropic except H2a. Only one of two crystallographically independent molecules is shown.

The electronic structure of Cp*$_2$TiH was investigated as part of an examination of the electronic structures of trivalent decamethyltitanocene complexes, Cp*$_2$TiX.[14] Although no EPR spectrum was observed at room temperature,[15] the EPR spectrum of Cp*$_2$TiH in frozen methylcyclohexane is rhombic with g_1 = 1.997, g_2 = 1.981, and g_3 = 1.780, and g_1 is a doublet with a coupling constant of 39 MHz (15 G) presumably due to coupling to the hydride proton.[16] In comparison, the EPR spectrum of Cp*$_2$TiCl is more isotropic with g_1 = 1.999, g_2 = 1.984, and g_3 = 1.889.[14,17] The electronic spectrum of Cp*$_2$TiH shows two absorptions in the visible region with energies of 20 980 and 18 270 cm^{-1} corresponding to the $1a_1 \rightarrow 2a_1$ and $1a_1 \rightarrow b_1$ transitions, respectively; the symmetry labels are those used by Lauher and Hoffmann.[10] These observations suggest that the mixing of the d_{z^2} and $d_{x^2-y^2}$ orbitals (where the x axis is the C_2 axis of the metallocene and the z axis is perpendicular to the plane formed by the titanium atom and the two Cp* centroids)[18] to form the $1a_1$ orbital occupied by the unpaired electron in Cp*$_2$TiH is much greater than the mixing in other trivalent decamethyltitanocenes.[14] The ratio of d_{z^2} to $d_{x^2-y^2}$ in Cp*$_2$TiH is 2, compared to a ratio of 13 in Cp*$_2$TiCl, this suggests that the molecular structure of Cp*$_2$TiH is different in some way from those of the other trivalent decamethyltitanocenes.[14] It was to test this postulate that the solid-state structure of Cp*$_2$TiH was determined.

Two crystallographically independent molecules exist in the asymmetric unit; one of which is shown in Figure 1. Crystal data are in Table 1, and selected distances and angles are reported in Table 2. The molecules differ only in the orientation of the Cp* rings. One of the

(11) de Wolf, J. M.; Meetsma, A.; Teuben, J. H. *Organometallics* **1995**, *14*, 5466.

(12) Girling, R. B.; Grebnik, P.; Perutz, R. N. *Inorg. Chem.* **1986**, *25*, 31.

(13) (a) Thompson, M. E.; Baxter, S. M.; Bulls, A. R.; Burger, B. J.; Nolan, M. C.; Santarsiero, B. D.; Schaefer, W. P.; Bercaw, J. E. *J. Am. Chem. Soc.* **1987**, *109*, 203. (b) Curtis, C. J.; Smart, J. C.; Robbins, J. L. *Organometallics* **1985**, *4*, 1283.

(14) Lukens, W. W., Jr.; Smith, M. R., III; Andersen, R. A. *J. Am. Chem. Soc.* **1996**, *118*, 1719.

(15) At room temperature, a weak resonance with g = 1.975 is observed. On the basis of the similarity of this value to that of Cp*$_2$TiOMe (g = 1.977),[17] this signal is thought to be due to Cp*$_2$TiOH or a similar species resulting from the reaction of Cp*$_2$TiH with advantitious water. Unfortunately, we have been unable to prepare pure Cp*$_2$TiOH to confirm this assignment.

(16) Although we have been unable to synthesize the deuteride, Cp*$_2$TiD, the perdeuterated analogue, (d_{15}-Cp*)$_2$TiD, does not show a splitting of g_1 because the expected coupling to deuterium of 2.3 G is smaller than the line width of 4 Hz. Other than the lack of splitting of g_1, the spectra of (d_{15}-Cp*)$_2$TiD and Cp*$_2$TiH are similar.

(17) Mach, K.; Raynor, B. *J. Chem. Soc., Dalton Trans.* **1992**, 683.

(18) (a) Petersen, J. L.; Dahl, L. F. *J. Am. Chem. Soc.* **1975**, *97*, 6416. (b) Petersen, J. L.; Dahl, L. F. *J. Am. Chem. Soc.* **1975**, *97*, 6422.

Table 1. Crystal Data

	Cp^*_2TiH	$Cp^*_2Ti(\mu\text{-}H)_2Li(tmed)$	$[Cp^*_2TiOLi(THF)]_2\cdot THF$
space group	*C*2/*c*	$Pna2_1$	$Pca2_1$
a, Å	44.9509(7)	18.911(2)	18.6055(3)
b, Å	8.4846(2)	8.563(2)	17.1084(3)
c, Å	22.7333(4)	17.460(3)	16.1954(2)
α, deg	90	90	90
β, deg	119.905(1)	90	90
γ, deg	90	90	90
V, Å^3	7515.8(3)	2678(1)	5155.2(1)
Z	16	4	4
fw	319.36	441.51	898.92
d(calcd), g cm^{-3}	1.129	1.095	1.158
μ(calcd), cm^{-1}	4.49	3.52	3.277
radiation		Mo Kα (λ = 0.710 73 Å)	
monochromator		highly oriented graphite	
data coverage	0.83 Å, 90%	$3° < 2\theta < 45°$	0.83 Å, 93%
scan speed	30 s per image	3.4 deg/min	30 s per image
scan type	ω, 0.3°	$\theta - 2\theta$	ω, 0.3°
reflections collected	16 761	2038 (+*h*,+,+*l*)	22 754
unique reflections	6740	1819	4862
R_{int}	0.043		0.059
reflections $I > 3\sigma(I)$	4528	1306 [$F_o^2 > 3\sigma(F_o^2)$]	3730
R, %	4.8	7.7	5.9
R_2, %	5.7	9.6	7.1
GOF	2.01	2.17	2.48

Table 2. Selected Distances (Å) and Angles (deg) in Cp^*_2TiH[a]

molecule 1		molecule 2	
Ti1−H1a	1.69(5)	Ti2−H2a	1.84(4)
Ti1−⟨C_{ring}⟩	2.36(1)	Ti2−⟨C_{ring}⟩	2.36(1)
Ti1−Cp1	2.03	Ti2−Cp3	2.03
Ti1−Cp2	2.03	Ti2−Cp4	2.04
Cp1−Ti1−Cp2	152.3	Cp3−Ti2−Cp4	152.0
Cp1−Ti1−H1a	103	Cp3−Ti2−H2a	106
Cp2−Ti1−H1a	104	Cp4−Ti2−H2a	101

[a] Cp1, Cp2, Cp3, and Cp4 are the centroids of the Cp* rings.

molecules has idealized C_2 symmetry while the other has idealized C_s symmetry. All of the hydrogen atoms in the molecules were located. The positions of the Cp* hydrogens were refined, and they were given one global, isotropic thermal parameter which was also refined. The hydridic hydrogens were refined isotropically. Given the facts that the independent Ti−H distances are the same to within 3σ, that little excess positive or negative electron density is present in the final difference Fourier map, and that titanium does not have a large number of electrons, we feel confident that the hydride positions are their true positions. The Ti−Cp*(centroid) distances and the Ti−C_{ring} distances are very similar to those in other trivalent decamethyltitanocene complexes.[14,19,20] In both independent molecules, the hydride atoms lie on the C_2 axis and have reasonable thermal parameters of 7(1) and 8(1) Å^2 for H1a and H2a, respectively. In addition, neither molecule shows any deviation toward a fulvene−dihydrogen complex.

The solid-state structure of Cp^*_2TiH is different from those of other Cp^*_2TiX complexes in one respect, viz., the Cp(centroid)−Ti−Cp(centroid) angle is opened by ca. 7° relative to Cp^*_2TiF and by ca. 15° relative to the other known Cp^*_2TiX derivatives. The origin of the open angle is most reasonably ascribed to the steric repulsions between the methyl groups on the "back" of the bent metallocene wedge. These methyl groups move closer to each other as the wedge angle decreases and move out of the plane defined by the cyclopentadienyl carbon atoms in order to minimize the steric repulsions. The small size of the hydride ligand relative to all of the other X ligands studied allows the wedge angle to be larger than normal without causing undue steric repulsion between the hydride ligand and the Cp* methyl groups at the "front" of the metallocene wedge. In the only other structurally characterized Cp_2MH compounds, $(Me_4PhC_5)_2TiH$[11] and $(Me_4EtC_5)CpReH$,[21] the Cp(centroid)−M−Cp(centroid) angles are also large.

The open metallocene angle in Cp^*_2TiH decreases the energy difference between the $1a_1$ and $2a_1$ orbitals, which allows greater hybridization (mixing) between the d_{z^2} and $d_{x^2-y^2}$ orbitals. In addition, the energy separation between the $1a_1$ orbital (where the unpaired electron resides) and the b_2 orbital is also small. This small energy gap is perhaps the reason that no EPR signal is observed for Cp^*_2TiH at room temperature.

Synthesis and Structure of $Cp^*_2Ti(\mu\text{-}H)_2Li(tmed)$. Addition of *n*-BuLi in tmed and hexane to a cold (−78 °C) solution of Cp^*_2TiH in hexane yields a green solution from which green crystals of $Cp^*_2Ti(\mu\text{-}H)_2Li(tmed)$ are obtained upon crystallization from diethyl ether in 70% yield. An identical compound may be obtained, in lower yield, by reducing Cp^*_2TiCl with $[Li(tmed)]_2C_{10}H_8$[22] in diethyl ether. The identification of this paramagnetic metallocene dihydride anion relies primarily upon its EPR spectrum because the hydride signature is not readily apparent in its infrared spectrum or in the X-ray structure.

The solid-state structure of the anion is shown in Figure 2. Selected bond distances and angles are given

(19) Luinstra, G. A.; Cate, L. C. T.; Heeres, H. J.; Pattiasina, J. W.; Meetsma, A.; Teuben, J. H. *Organometallics* **1991**, *10*, 3227.

(20) (a) Brady, E.; Lukens, W.; Telford, J.; Mitchell, G. *Acta Crystallogr.* **1994**, *C51*, 558. (b) Feldman, J.; Calabrese, J. C. *J. Chem. Soc., Chem. Commun.* **1991**, 1042. (c) Pattiasina, J. W.; Heeres, H. J.; van Bolhuis, F.; Meetsma, A.; Teuben, J. H. *Organometallics* **1987**, *6*, 1004.

(21) Paciello, R. A.; Kiprof, P.; Herdtweck, E.; Herrmann, W. A. *Inorg. Chem.* **1989**, *28*, 2890.

(22) (a) Brooks, J. J.; Rhine, W.; Stucky, G. D. *J. Am. Chem. Soc.* **1972**, *94*, 7346. (b) Kahn, B. E.; Rieke, R. D. *Organometallics* **1988**, *7*, 463.

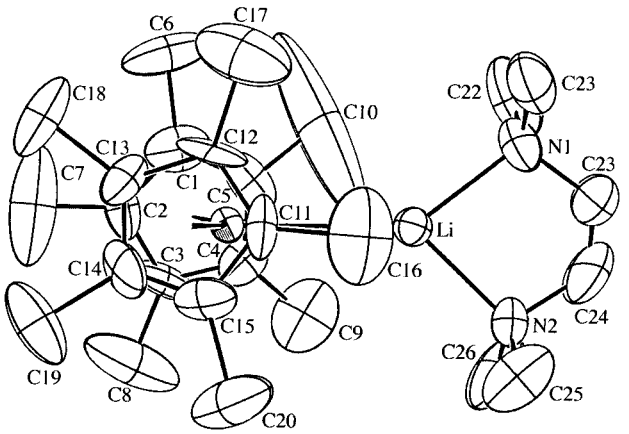

Figure 2. ORTEP diagram of Cp*$_2$Ti(μ-H)$_2$Li(tmed), 50% thermal ellipsoids. The hydrogen atoms are not located.

in Table 3, and crystal data are listed in Table 1. Although the quality of the structure is low due to disorder in the tmed ligand and in one of the Cp* ligands, the general connectivity is defined beyond doubt. The structural features of the Cp*$_2$Ti and Li(tmed) fragments are not unusual in any way. The Cp*(centroid)−Ti distance of 2.05 Å and the Cp*(centroid)−Ti−Cp*(centroid) angle of 145° are normal for trivalent decamethyltitanocenes.[14,19,20] The Li−N distance of 2.16(1) Å (av) and the N−Li−N angle of 82.1(9)° in the Li(tmed) fragment are similar to those found in [Li(tmed)]$_2$Ni(norbornene)$_2$,[23] [Li(tmed)]$_2$Ni(cyclododecatriene),[24] and MeH$_4$C$_5$[Li(tmed)]$_2^-$.[25] The Ti···Li distance is 2.94(2) Å. Although the hydride atoms are not located in the X-ray diffraction experiment, it is not unreasonable to place them on either side of the Ti···Li vector because ample room exists for them. An idealized drawing of the molecule is shown below, and the Ti(μ-H)$_2$Li geometry displayed there is similar to that found in the magnesium hydride complex, Cp*$_2$Ti(μ-H)$_2$Mg(μ-H)$_2$TiCp*$_2$, where the hydrides were located in bridging sites between the Ti and Mg atoms; the Ti···Mg distance is 2.860(4) Å.[26]

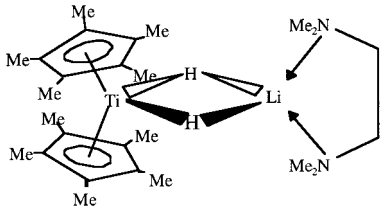

With the heavy-atom structure and overall molecular geometry defined, the magnetism and EPR spectrum can be used to resolve the details of oxidation state and stoichiometry. The variable-temperature magnetic susceptibility of the dihydride anion follows Curie−Weiss behavior from 5 to 300 K with $\mu_{eff} = 1.75\mu_B$ and $\theta = -5.3$ K at 5 and 40 kG. In benzene solution, $\mu_{eff} = 1.7\mu_B$ at 303 K as determined by Evans' method. The magnetic susceptibility is unequivocal; the complex has a single unpaired electron, and the titanium is trivalent, as in the starting hydride, Cp*$_2$TiH. The most reasonable formulation then is a dihydride anion, Cp*$_2$TiH$_2^-$. The room-temperature EPR spectrum and simulation of this complex in methylcyclohexane is consistent with this assertion. A complex spectrum, centered at $g = 1.989$, is shown in Figure 3a. The simulation consists of two species; the first species (^{7}Li) has 92.5% of the total area and a 9.29 G coupling to two-spin $^1/_2$ nuclei and a 2.8 G coupling to one-spin $^3/_2$ nucleus, and the second species (^{6}Li) has 7.5% of the total area and a 9.47 G coupling to two-spin $^1/_2$ nuclei and a 0.7 G coupling to one-spin 1 nucleus. The pattern is greatly simplified by replacing ^{7}Li ($I = {}^3/_2$, $g = 10.396$) with ^{6}Li ($I = 1$, $g = 3.397$) as shown in Figure 3b. The triplet feature in the simulation of the latter EPR spectrum is due to interaction of the unpaired electron with two equivalent hydrogen atoms with $A_H^{iso} = 9.56$ G; the 0.78 G coupling to ^{6}Li is not resolved because of the line width of 2 G. In comparison, for Cp$_2$Ti(μ-H)$_2$Li(THF), A_H^{iso} is 9.6 G and A_{Li}^{iso} is 2.3 G.[3]

The anion may be reasonably suggested to be produced by β elimination from the hypothetical intermediate Cp*$_2$Ti(H)(*n*-Bu)$^-$ which results from addition of Li−*n*-Bu to Cp*$_2$TiH. This is also presumably the pathway by which the original dihydride anions were

Table 3. Distances and Angles in Cp*$_2$Ti(μ-H)$_2$Li(tmed)[a]

distances (Å)		angles (deg)	
Ti−Li	2.94(2)	Cp1−Ti−Cp2	145.2
Ti−Cp1	2.05	Cp1−Ti−Li	107.9(4)
Ti−Cp2	2.05	Cp2−Ti−Li	106.7(4)
Ti−⟨C$_{ring}$⟩	2.36(4)	Ti−Li−N1	142(1)
Li−N1	2.15(3)	Ti−Li−N2	136(1)
Li−N2	2.18(2)	N1−Li−N2	82.1(9)

[a] Cp1 and Cp2 are the centroids of the Cp* rings.

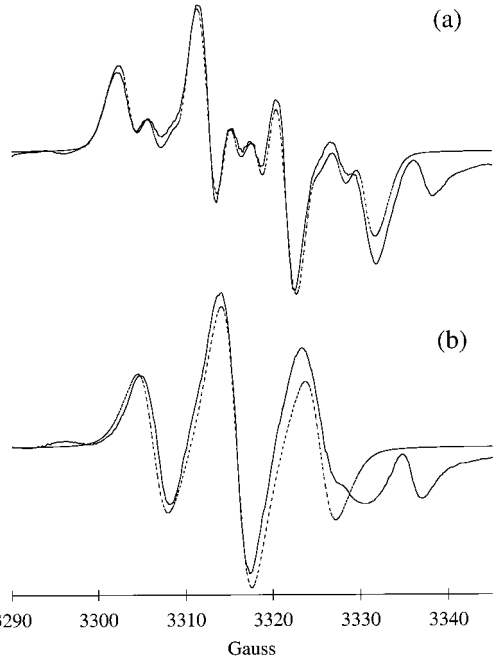

Figure 3. Room-temperature EPR spectra (solid lines) and simulations (dotted lines) of (a) Cp*$_2$Ti(μ-H)$_2$Li(tmed) and (b) Cp*$_2$Ti(μ-H)$_2$^{6}Li(tmed).

(23) Jonas, K.; Schieferstein, L. *Angew. Chem., Int. Ed. Engl.* **1976**, *15*, 47.
(24) Brauer, D. J.; Krüger, C.; Sekutowski, J. C. *J. Organomet. Chem.* **1979**, *178*, 249.
(25) Stults, S. D.; Andersen, R. A.; Zalkin, A. *J. Am. Chem. Soc.* **1989**, *111*, 4507.
(26) Troyanov, S. I.; Varga, V.; Mach, K. *J. Chem. Soc., Chem. Commun.* **1993**, 1174.

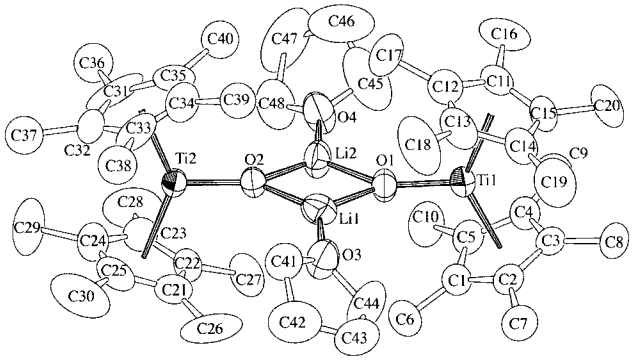

Figure 4. ORTEP diagram of $[Cp^*_2TiOLi(THF)]_2$, 50% thermal ellipsoids, all atoms anisotropic.

Table 4. Distances (Å) and Angles (deg) in $[Cp^*_2TiOLi(THF)]_2 \cdot THF$[a]

titanium 1		titanium 2	
Ti1−O1	1.783(4)	Ti2−O2	1.791(4)
Ti1−Cp1	2.16	Ti1−Cp3	2.14
Ti1−Cp2	2.14	Ti1−Cp4	2.14
Ti1−⟨C_{ring}⟩	2.47(4)	Ti2−⟨C_{ring}⟩	2.45(4)
Li1−O1	1.88(1)	Li2−O1	1.88(1)
Li1−O2	1.87(1)	Li2−O2	1.84(1)
Li1−O3	1.92(1)	Li2−O4	1.95(1)
Ti1−Ti2	6.111(2)	Li1−Li2	2.29(2)
Cp1−Ti1−Cp2	137.5	Cp3−Ti2−Cp4	138.4
Cp1−Ti1−O1	111.0	Cp3−Ti2−O2	110.9
Cp2−Ti1−O1	111.5	Cp4−Ti2−O2	110.7
Ti1−O1−Li1	141.6(5)	Ti2−O2−Li1	142.2(4)
Ti1−O1−Li2	143.0(4)	Ti2−O2−Li2	141.5(5)
O1−Li1−O2	103.7(6)	O1−Li2−O2	105.2(7)
O1−Li1−O3	125.6(7)	O1−Li2−O4	125.4(6)
O2−Li1−O3	130.3(6)	O2−Li2−O4	129.2(7)

[a] Cp1, Cp2, Cp3, and Cp4 are the centroids of the Cp* rings.

derived.[2,3] The origin of the hydride ligands in the reaction of Cp^*_2TiCl with $[Li(tmed)]_2C_{10}H_8$ is unknown.

Synthesis and Structure of $Cp^*_2TiOLi(THF)$ Dimer. The addition of a slight excess of water in THF to the dihydride anion at −78 °C gives a light green solution from which a compound of the empirical composition $Cp^*_2TiOLi(THF)_{1.5}$ crystallizes as green truncated pyramids. The paramagnetic (see below) compound does not melt and does not give a molecular ion in the electron impact mass spectrum. It reacts with MeI to give Cp^*_2TiOMe as the only paramagnetic species detected by EPR. This information indicates that the titanium atom is trivalent, so the tentative formulation as a metallocene−oxo anion $Cp^*_2TiO^-$, isoelectronic with Cp^*_2TiF, can be advanced.

The structure of the molecule is shown in Figure 4. Selected bond distances and angles are given in Table 4, and crystal data are reported in Table 1. One of the Cp* ligands is disordered (C31−C35); this disorder is modeled using two sets of methyl groups as described in the Experimental Section. An additional molecule of THF is present in the asymmetric unit but is not associated with the metallocene dimer. The molecule is a noncentrosymmetric dimer formed by bridging together two $Cp^*_2TiO^-$ fragments with two Li(THF) fragments. The O_2Li_2 core is roughly square with opposite vertexes occupied by O or Li. The planes defined by Cp*(centroid)−Ti−Cp*(centroid) are nearly coincident (Figure 5). The Cp* rings are oriented to minimize steric interactions among Cp* ligands on

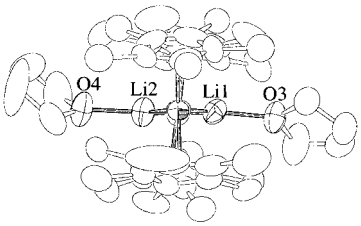

Figure 5. ORTEP diagram of $[Cp^*_2TiOLi(THF)]_2$ showing the view down the Ti···Ti vector.

adjacent Ti centers, and the dimer has idealized C_{2h} symmetry. This molecule is very unusual because all other decamethyltitanocenes are monomeric in the solid state, with the notable exception of $(Cp^*_2Ti)_2(\mu\text{-}N_2)$ in which the two metallocene fragments are oriented orthogonal to each other apparently to minimize steric interactions caused by the short Ti···Ti separation.[27] The oxoanion cannot have a similar orientation of the Cp^*_2Ti fragments because this orientation would result in severe THF···Cp* ring repulsions for two of the Cp* ligands. The observed stereochemistry of $[Cp^*_2TiOLi(THF)]_2$ minimizes all intramolecular steric interactions even though the dimer is quite sterically crowded. This crowding is reflected in the bond parameters of the $Cp^*_2TiO^-$ fragment. The Cp*(centroid)−Ti distance of 2.15 Å is longer than the distance normally found in monomeric Cp^*_2TiX molecules, which ranges from 2.06 to 2.09 Å, and the Cp*(centroid)−Ti−Cp*(centroid) angle of 138° is slightly less than that usually found; the normal range is 140−145°.[14,19,20]

Two specific structural comparisons between related titanium metallocenes with oxygen or fluorine ligands further illuminate these generalities. As noted above, fluorine is isoelectronic with the oxygen monoanion, and the Ti−X bond lengths in Cp^*_2TiF and $Cp^*_2TiO^-$ are similar; see Table 5. The Ti−X distances are nearly identical when adjusted for the smaller size of O^{2-} relative to F^-.[28] In these two molecules, the Cp*(centroid)−Ti−X angles are similar, but the Ti−Cp*(centroid) distance is longer, and the Cp*(centroid)−Ti−Cp*(centroid) angle is smaller in the oxo−metallocene anion. Presumably, this is due to repulsions between ligands on adjacent metal centers as mentioned earlier. The unsubstituted dinuclear oxo compound, $(Cp_2Ti)_2(\mu\text{-}O)$,[29] in which the Cp_2Ti fragments are orthogonal to each other, has a Ti−O distance identical to the Ti−F distance in Cp^*_2TiF, but it is slightly longer than that found in the oxo dimer, in which the oxygen ligand has a formal negative charge. In addition, the Cp(centroid)−Ti−Cp(centroid) and Cp(centroid)−Ti−O angles in $(Cp_2Ti)_2(\mu\text{-}O)$ and $[Cp^*_2TiOLi(THF)]_2$ are identical, but the Cp(centroid)−Ti distance in the Cp* derivative is ca. 0.1 Å longer; see Table 5. These changes presumably reflect how these two Ti(III) oxo compounds respond to the steric repulsions caused by changing from Cp to Cp*.

The Li_2O_2 unit in $[Cp^*_2TiOLi(THF)]_2$ strongly resembles those of dimeric alkoxides of the type [ROLi-

(27) Sanner, R. D.; Duggen, D. M.; McKenzie, T. C.; Marsh, R. E.; Bercaw, J. E. *J. Am. Chem. Soc.* **1976**, *98*, 8358.

(28) Robinson, E. A.; Johnson, S. A.; Tang, T.-H.; Gillespie, R. J. *Inorg. Chem.* **1997**, *36*, 3022.

(29) (a) Honold, B.; Thewalt, U.; Herberhold, M.; Alt, H. G.; Kool, L. B.; Rausch, M. D. *J. Organomet. Chem.* **1986**, *314*, 105. (b) Lukens, W. W.; Andersen, R. A. *Inorg. Chem.* **1995**, *34*, 3440.

Table 5. Comparison of Selected Bond Parameters in Titanocenes

compound	Ti−Cp(centroid) (Å)	Cp(centroid)−Ti−Cp(centroid) (deg)	Cp(centroid)−Ti−X (deg)	Ti−X (Å)	reference
[Cp*$_2$TiOLi(THF)]$_2$	2.15	138	111	1.787(3)	this work
Cp*$_2$TiF	2.06	145	108	1.841(2)	14
(Cp$_2$Ti)$_2$(μ-O)	2.07	136	112	1.838(1)	29a

(ether)]$_2$. In the dimers where R is 2,6-di-*tert*-butylphenyl or tris-*tert*-butylmethyl and ether is either diethyl ether or THF, the Li_2O_2 have bond lengths and angles identical to those in [Cp*$_2$TiOLi(THF)]$_2$.[30−32]

The room-temperature EPR spectrum of the dimer consists of a single line at $g = 1.982$. The isotropic g value can be used as a gauge of π bonding in monomeric, trivalent decamethyltitanocenes.[14] If assumptions made for the monomer also hold true for the dimer, then the large value of g_{av} is consistent with substantial Ti−O π bonding in the anion. The degree of π bonding is comparable to that in Cp*$_2$TiNH$_2$ or Cp*$_2$TiN(H)Me, which is consistent with our intuition.

The variable-temperature magnetic susceptibility follows the Curie−Weiss law from 5 to 300 K at 5 and 50 kG with $\mu = 2.45\mu_B$ per dimer or $1.73\mu_B$ per titanium. The magnetic susceptibility reveals that no coupling occurs between unpaired electrons on adjacent titanium centers. Therefore, as in (Cp$_2$Ti)$_2$(μ-O),[29] no superexchange pathway exists. Along with the absence of coupling to lithium in the EPR spectrum, the lack of a superexchange pathway supports the structural model advanced earlier; namely, the dimer consists of two isolated Cp*$_2$TiO$^-$ fragments linked together by the two Li(THF) fragments. The orbital symmetry diagram for the titanium fragment is related to that developed for (Cp$_2$Ti)$_2$(μ-O).[29] The single electron is in the $1a_1$ orbital, and it is no surprise that the magnetic moments of these two dinuclear complexes are similar.

Experimental Section

All reactions and manipulations were carried out in an inert atmosphere using standard Schlenk and drybox techniques. Hexane, diethyl ether, and THF were dried over sodium benzophenone ketyl and distilled and degassed immediately prior to use. Toluene, methylcyclohexane, and deuterated NMR solvents were dried over and distilled from potassium or sodium.

Infrared spectra were recorded on a Perkin-Elmer 283 spectrometer as Nujol mulls between CsI plates. ^{1}H NMR spectra were measured on a JEOL FX-90Q FT NMR spectrometer operating at 89.56 MHz. Chemical shifts were referenced to tetramethylsilane ($\delta = 0$) with positive values at lower field. All spectra were acquired at 30 °C in C_6D_6. Melting points were measured on a Thomas-Hoover melting point apparatus in sealed capillaries and are uncorrected. EPR spectra were measured as solutions or frozen glasses using a Varian E-12 spectrometer. The microwave frequency was measured using an EIP-548 microwave frequency counter, and the magnetic field was measured using a Varian E-500 NMR gaussmeter. Spectra were digitized using UNPLOTIT or UNSCANIT. EPR spectra were fit using the program PEST WinSim.[33] Susceptibility measurements were carried out on a SHE model 500 SQUID susceptometer. All calculations and numerical modeling of susceptibilities were done using the program Horizon. Electron impact mass spectra were recorded by the mass spectroscopy laboratory, and elemental analyses were performed by the analytical laboratories; both laboratories are at the University of California, Berkeley.

Cp*$_2$TiH. A solution of Cp*$_2$TiMe[19] (0.86 g, 2.6 mmol) in pentane (15 mL) was placed into a thick-walled pressure bottle and stirred under hydrogen (10 atm) for 2 h. The resulting red solution was concentrated and cooled to −40 °C, yielding deep red plates (0.79 g, 96%). Mp: 234−237 °C. IR: 2768(w), 2725(m), 1512(s), 1489(s), (Ti−H; 1048, Ti−D), 1436(sh), 1261(w), 1161(w), 1099(w), 1064(w), 1023(s), 827(m), 800(m), 722(w), 614(w), 571(m), 460(s), 436(w), 407(w), 296(m) cm^{-1}. ^{1}H NMR (C_7D_8, 30 °C): δ 22.64 ($\nu_{1/2} = 128$ Hz). MS m/z: (M − H)$^+$ 317. Anal. Calcd for $C_{20}H_{31}Ti$: C, 75.2; H, 9.78. Found: C, 75.3; H, 9.84.

Cp*$_2$Ti(μ-H)$_2$Li(tmed). (A) A mixture of Cp*$_2$TiCl[20c] (1.00 g, 2.83 mmol) and [(tmed)Li]$_2$C$_{10}$H$_8$[22] (1.08 g, 2.88 mmol) was cooled to −78 °C and powdered using a stirbar. The solid mixture was suspended in 100 mL of cold diethyl ether, and the solution was allowed to warm to room temperature as it was stirred. After it was stirred for 1 h at room temperature, the solution was green with a green precipitate. The diethyl ether was removed under reduced pressure. The dark green solid residue was heated to 95 °C under vacuum for 2 h to remove $C_{10}H_8$ and then suspended in 200 mL of diethyl ether. The mixture was heated to reflux and allowed to cool and settle. The dark red solution was filtered, and the volume of the filtrate was reduced to ca. 40 mL. Cooling to −20 °C produced dark green, blade-shaped crystals (0.48 g, 38%). The compound did not melt at or below 300 °C. IR: 2715(w), 1365(w), 1290(m), 1250(s), 1185(w), 1160(m), 1130(s), 1100(m), 1040(m), 1020(s), 950(s), 890(w), 840(w), 795(s), 725(m), 630(w), 505(w), 470(w), 445(m), 410(s), 255(w) cm^{-1}. Anal. Calcd for $C_{26}H_{48}LiN_2Ti$: C, 70.3; H, 10.9; N, 6.30. Found: C, 70.7; H, 10.6; N, 6.07.

(B) Cp*$_2$TiH (0.28 g, 0.88 mmol) was dissolved in 50 mL of hexane and cooled to −78 °C. A mixture of tmed (0.15 mL, 0.11 g, 0.96 mmol) and *n*-BuLi (0.49 mL, 1.97 M in hexane, 0.96 mmol) was cooled to −78 °C, dissolved in 30 mL of hexane, and added to the solution of Cp*$_2$TiH. The red solution immediately turned emerald green, and it was allowed to warm to room temperature. After being stirred for 1 h, the volatile components were removed under reduced pressure, and the green solid residue was suspended in 100 mL of diethyl ether. The solution was heated to reflux briefly and then allowed to settle. The green solution was filtered, and the volume of the filtrate was reduced to ca. 40 mL. Cooling to −20 °C produced dark green blades (0.25 g, 69%). The EPR spectrum and appearance of the compound is identical to that of compound prepared by route A.

[Cp*$_2$TiOLi(THF)]$_2$·THF. Cp*$_2$Ti(μ-H)$_2$Li(tmed) (0.50 g, 1.1 mmol) was dissolved in 30 mL of THF and cooled to −78 °C. A solution of degassed water (20.4 mL, 1.13 mmol) in 30 mL of THF was added by cannula. The solution turned a lighter green color and evolved gas over the course of 3 h. After being stirred for 12 h, green solid had precipitated. An additional 100 mL of THF was added, the mixture was heated to 80 °C, and then was allowed to cool to room temperature. The solution was filtered, the volume of the filtrate was reduced to ca. 90 mL, and the filtrate was heated to 80 °C to

(30) Kodiok-Köhn, G.; Pickardt, J.; Schumann, H. *Acta Crystallogr.* **1991**, *C47*, 2649.

(31) Huffman, J. C.; Geerts, R. L.; Caulton, K. G. *J. Cryst. Spectrosc. Res.* **1984**, *14*, 541.

(32) Hvoslef, J.; Hope, H.; Murray, B. D.; Power, P. P. *J. Chem. Soc., Chem. Commun.* **1983**, 1438.

(33) Duling, D. R. *J. Magn. Reson.* **1994**, *B104*, 105. Available from the NIEHS EPR website at hippo.niehs.nih.gov.

dissolve the solid. Cooling to −20 °C produced large green prisms (0.27 g, 53%). The compound does not melt at or below 250 °C. IR: 2720(w), 1600(w), 1020(m), 800(w), 705(s), 625-(m), 610(m), 410(s), 370(w), 305(w) cm^{-1}. Anal. Calcd for $C_{52}H_{84}Li_2O_5Ti$: C, 69.5; H, 9.42. Found: C, 69.6; H, 9.53. Adding MeI to the EPR sample produces Cp^*_2TiOMe (g = 1.977).[14]

Crystallography. Cp^*_2TiH. Red crystals of the compound were grown by cooling a hexane solution to −20 °C. The crystals were placed in Petri dish of Paratone N in a glovebag. A suitable irregularly shaped crystal measuring 0.26 × 0.20 × 0.20 mm was mounted on the end of a 0.2-mm thin-walled glass capillary. The crystal was transferred to a Siemens SMART diffractometer and cooled to −137 °C under a cold stream previously calibrated by a thermocouple placed in the sample position. The crystal was centered in the beam. Automatic peak search and indexing procedures indicated that the crystal possessed a C-centered monoclinic cell and yielded the unit cell parameters. The cell parameters and data collection parameters are given in Table 1. On the basis of a statistical analysis of intensity distribution and the successful solution and refinement of the crystal structure, the space group was found to be *C*2/*c*.

An arbitrary hemisphere of data was collected using the default parameters for the diffractometer. The data were collected as 30-s images with an area detector. Two images were averaged to give the net image data. The image data were integrated using the program SAINT. The 16 761 raw intensity data were converted to structure-factor amplitudes and their esd's by correction for scan speed, background, and Lorentz polarization effects.[34] Inspection of the intensity standards showed no decrease in intensity over the duration of data collection. Because of the small value of μ, no absorption correction was used. Averaging equivalent reflections gave 6740 unique data (R_{int} = 0.043).

The titanium-atom positions were obtained by direct methods. Refinement on the titanium positions followed by a difference Fourier search yielded the other heavy-atom positions. The heavy-atom structure was refined by standard least-squares and Fourier techniques. The heavy atoms were refined with anisotropic thermal parameters. The Cp* hydrogen positions were refined with all thermal parameters equal to 4.98 Å^2. The hydrides were refined with isotropic thermal parameters. Toward the end of the refinement, examination of the extinction-test listing indicated that secondary extinction was occurring. The secondary extinction coefficient was refined to 5.37 × 10^{-8}. A final difference Fourier map showed no additional atoms in the asymmetric unit. No close (<3.5 Å) intermolecular contacts were found.

The final residuals for 568 variables refined against the 4528 unique data with $I > 3\sigma(I)$ were R = 4.8%, R_w = 5.7%, and GOF = 2.01. The quantity minimized by the least-squares refinements was $w(|F_o| - |F_c|)^2$, where w is the weight given to a particular reflection. The p factor, used to reduce the weight of intense reflections, was set to 0.03.[35] The analytical forms of the scattering factor tables for neutral atoms were used, and all non-hydrogen scattering factors were corrected for both the real and imaginary components of anomalous dispersion.[36]

Inspection of the residuals ordered in the ranges of sin(θ/λ), $|F_o|$, and parity and values of the individual indexes showed no trends other than the previously mentioned secondary extinction. No reflections had anomalously high values of $w \times \Delta^2$. The largest positive and negative peaks in the final difference Fourier map have electron densities of 0.30 and −0.33 e Å^{-3}, respectively. The software package TeXsan was used for structure solution and refinement.[37]

$Cp^*_2Ti(\mu\text{-}H)_2Li(tmed)$. Dark purple-black crystals of the compound were grown by cooling a saturated ether solution to −30 °C. The crystals were dried in vacuo and taken into an inert-atmosphere box. They were then placed in a small Petri dish and covered with Paratone N, a high molecular weight hydrocarbon oil. A blade-shaped single crystal was selected, and a wedge-shaped piece measuring 0.45 × 0.40 × 0.40 mm was cut out of the middle. The crystal was mounted on the end of a 0.4-mm-diameter quartz capillary with a drop of Paratone N. The crystal was transferred to an Enraf-Nonius CAD-4 diffractometer and cooled to −89 °C under a cold stream of nitrogen gas previously calibrated by a thermocouple placed in the sample position. The crystal was centered in the beam. Automatic peak search and indexing procedures indicated that the crystal possessed a primitive orthorhombic cell and yielded the cell parameters. The cell parameters and data collection parameters are given in Table 1. Reflections (4,1,7), (2,8,6), and (1,5,9) were checked after every 200 measurements. Crystal orientation was redetermined if any of the reflections were offset from their predicted positions by more than 0.1°. Reorientation was required twice over the course of the data collection.

The 2038 raw intensity data were converted to structure-factor amplitudes and their esd's by correction for scan speed, background, and Lorentz polarization effects.[34] Inspection of the intensity standards showed a large dip of 25% between hours 1 and 4, presumably due to a slight movement of the crystal. A nonlinear decay correction was applied. The 219 systematic absences (h,0,l), h odd, and (0,k,l), $k + l$ odd, were then rejected, yielding 1819 unique data of which 1306 possessed $F_o > 3\sigma(F_o)$. Azimuthal scan data showed a difference of I_{min}/I_{max} = 0.68 for the averaged curve; however, the different reflections had different absorption curves. No empirical absorption correction was applied. The systematic absences indicated that the space group was $Pna2_1$ or $Pnma$. Because the molecule would have to sit on a special position and possess mirror symmetry in $Pnma$ (which seemed un-

(34) The data reduction formulas are

$$F_o^2 = \frac{\omega}{\mathrm{Lp}}(C - 2B)$$

$$\sigma_o(F_o^2) = \frac{\omega}{\mathrm{Lp}}(C + 4B)^{1/2}$$

$$F_o = (F_o^2)^{1/2}$$

$$\omega_o(F) = [F_o^2 + \sigma_o(F_o^2)]^{1/2} - F_o$$

where C is the total count of the scan, B is the sum of the two background counts, ω is the scan speed used in deg/min, and

$$\frac{1}{\mathrm{Lp}} = \frac{\sin 2\theta(1 + \cos^2 2\theta_m)}{1 + \cos^2 2\theta_m - \sin^2 2\theta}$$

is the correction for Lorentz and polarization effects for a reflection with scattering angle 2θ and radiation monochromatized with a 50% perfect single-crystal monochromator with scattering angle 2θ_m.

(35)
$$R = \frac{\sum ||F_o| - |F_c||}{\sum |F_o|} \qquad wR = \left[\frac{\sum (|F_o| - |F_c|)^2}{\sum wF_o^2}\right]^{1/2}$$

$$\mathrm{GOF} = \left[\frac{\sum (|F_o| - |F_c|)^2}{(n_o - n_N)}\right]^{1/2}$$

where n_o is the number of observations and n_v is the number of variable parameters, and the weights were given by

$$w = \frac{1}{\sigma^2(F_o)}\sigma(F_o^2)$$

$$= [\sigma_o^2(F_o^2) + (pF^2)^2]^{1/2}$$

where $\sigma^2(F_o)$ is calculated as above from $\sigma(F_o^2)$ and p is the factor used to lower the weight of intense reflections.

(36) Cromer, D. T.; Waber, J. T. In *International Tables for X-ray Crystallography*; Kynoch Press: Birmingham, England, 1974; Vol. IV.

(37) TeXsan, Molecular Structure Corp.; 1985.

likely), $Pna2_1$ was chosen. This choice is supported by the observations that (a) the molecule does not have mirror symmetry and (b) the mirror symmetry would have to be about the *z* axis, meaning that Ti, Li, and the two Cp centroids would have to have atomic positions with $z = 0$; this is not observed.

The cell volume indicated that four molecules were present in the unit cell. The titanium-atom position was obtained by solving the Patterson map. Successive Fourier searches yielded the rest of the heavy-atom positions. The heavy-atom structure was refined by standard least-squares and Fourier techniques. The heavy atoms were refined isotropically, and the hydrogen positions were then calculated based upon idealized bonding geometry and assigned thermal parameters equal to 1.5 $Å^2$ larger than those of the carbon atom to which they were connected. A numerical absorption correction, DIFABS, was then used. The heavy atoms, except for the lithium atom, were then refined anisotropically. One of the methyl carbon atoms of the Cp* ring has a very large thermal parameter, and the tmed group and one of the Cp* groups are disordered. The disorder was not modeled. At the end of the refinement, the enantiomer was changed and the structure refined. The refinement was very slightly worse, so the enantiomer was changed back to the original one. A final difference Fourier map showed no additional atoms in the asymmetric unit. Examination of intermolecular close contacts (<3.5 Å) showed that the molecule was a monomer.

The final residuals for 265 variables refined against the 1306 unique data with $F_o > 3\sigma(F_o)$ were $R = 7.73\%$, $R_w = 9.59\%$, and GOF = 2.166. The *R* value for all data (including unobserved reflections) was 11.28%. The quantity minimized by the least-squares refinements was $w(|F_o| - |F_c|)^2$, where *w* is the weight given to a particular reflection. The *p* factor, used to reduce the weight of intense reflections, was set to 0.03 initially but later changed to 0.07.[35] The analytical forms of the scattering factor tables for neutral atoms were used, and all non-hydrogen scattering factors were corrected for both the real and imaginary components of anomalous dispersion.[36]

Inspection of the residuals ordered in the ranges of $\sin(\theta/\lambda)$, $|F_o|$, and parity and values of the individual indexes showed no trends. Eleven reflections had anomalously high values of $w \times \Delta^2$ and were weighted to zero toward the end of the refinement. The largest positive and negative peaks in the final difference Fourier map have electron densities of 0.51 and −0.49 e $Å^{-3}$, respectively, and are associated with the one of the Cp* rings. The software package MOLEN was used for structure solution and refinement.[38]

$[Cp^*_2TiOLi(THF)]_2$·THF. Green crystals of the compound were grown by cooling a THF solution of the compound to −20 °C. The crystals were placed in Petri dish of Paratone N in a glovebag. A suitable irregularly shaped crystal measuring 0.30 × 0.35 × 0.40 mm was mounted on the end of a 0.3-mm thin-walled quartz capillary. The crystal was transferred to an Siemens SMART diffractometer and cooled to −100 °C under a cold stream previously calibrated by a thermocouple placed in the sample position. The crystal was centered in the beam. Automatic peak search and indexing procedures indicated that the crystal possessed a primitive orthorhombic cell and yielded the unit cell parameters. The cell parameters and data collection parameters are given in Table 1. On the basis of a statistical analysis of intensity distribution and the successful solution and refinement of the crystal structure, the space group was found to be $Pca2_1$.

(38) MOLEN, Enraf-Nonius Corp., 1990.

An arbitrary hemisphere of data was collected using the default parameters for the diffractometer. The data were collected as 30-s images with an area detector. Two images were averaged to give the net image data. The image data were integrated to give the intensity data using the program SAINT. The 22 754 raw intensity data were converted to structure-factor amplitudes and their esd's by correction for scan speed, background, and Lorentz polarization effects.[34] An empirical absorption correction using an ellipsoidal model for the crystal was applied to the intensity data based upon the intensities of all intense equivalent reflections ($T_{max} = 0.969$, $T_{min} = 0.863$). Inspection of the intensity standards showed no decrease in intensity over the duration of data collection. Averaging equivalent reflections gave 4862 unique data ($R_{int} = 0.059$).

The structure was solved by direct methods. The molecule was found to be a dimer with a THF molecule of crystallization. The heavy-atom structure was refined by standard least-squares and Fourier techniques. Most of the heavy atoms were refined with anisotropic thermal parameters. One of the Cp* ligands was found to be severely disordered. The disorder was modeled using two sets of Cp* methyl carbon atoms whose net occupancy (for related atoms) was 1. The hydrogen atoms were placed in calculated positions and included in structure-factor calculations but were not refined. A final difference Fourier map showed no additional atoms in the asymmetric unit. No close (<3.5 Å) intermolecular contacts were found.

The final residuals for 545 variables refined against the 3730 unique data with $I > 3\sigma(I)$ were $R = 5.9\%$, $R_w = 7.1\%$, and GOF = 2.48. The quantity minimized by the least-squares refinements was $w(|F_o| - |F_c|)^2$, where *w* is the weight given to a particular reflection. The *p* factor, used to reduce the weight of intense reflections, was set to 0.03 but was later increased to 0.04.[35] The analytical forms of the scattering factor tables for neutral atoms were used, and all non-hydrogen scattering factors were corrected for both the real and imaginary components of anomalous dispersion.[36]

Inspection of the residuals ordered in the ranges of $\sin(\theta/\lambda)$, $|F_o|$, and parity and values of the individual indexes showed no trends. No reflections had anomalously high values of $w \times \Delta^2$. The largest positive and negative peaks in the final difference Fourier map have electron densities of 0.31 and −0.38 e Å, respectively. The software package TeXsan was used for structure solution and refinement.[37]

Acknowledgment. The authors thank Dr. F. R. Hollander for assistance in crystal-structure analysis. W.W.L. thanks the National Science Foundation for a graduate fellowship. This work was partially supported by the Director, Office of Energy Research, Office of Basic Energy Sciences, Chemical Sciences Division of the U.S. Department of Energy under Contract No. DE-AC03-76SF00098.

Supporting Information Available: Tables of positional parameters and thermal parameters for Cp^*_2TiH, $Cp^*_2Ti(\mu\text{-}H)_2Li(tmed)$, and $[Cp^*_2TiOLi(THF)]_2$ (20 pages). This material is contained in many libraries on microfiche, immediately follows this article in the microfilm version of this journal, and can be ordered from ACS; see any current masthead page for ordering information. Tables of structure factors are available from the author.

OM980601N